Spirobifluorene Regioisomerism: A Structure–Property Relationship Study

— **Source link** ↗

Lambert Sicard, Cassandre Quinton, Jean-David Peltier, Denis Tondelier ...+6 more authors

Institutions: University of Rennes, Université Paris-Saclay, École normale supérieure de Cachan

Related papers:

- Structure–property relationship of 4-substituted-spirobifluorenes as hosts for phosphorescent organic light emitting diodes: an overview

- Spiro Compounds for Organic Optoelectronics

- ortho-, meta-, and para-dihydroindenofluorene derivatives as host materials for phosphorescent OLEDs.

- Dihydroindenofluorene Positional Isomers.

- C1-Linked Spirobifluorene Dimers: Pure Hydrocarbon Hosts for High-Performance Blue Phosphorescent OLEDs

Spirobifluorene Regioisomerism: A Structure–Property Relationship Study

Lambert Sicard, Cassandre Quinton, Jean-David Peltier, Denis Tondelier, Bernard Geffroy, Urelle Biapo, Rémi Métivier, Olivier Jeannin, Joëlle Rault-Berthelot, Cyril Poriel, et al.

Spirobifluorene regioisomerism: A structure-properties relationship study

*Lambert Sicard,[a] Cassandre Quinton,[a] Jean-David Peltier,[a] Denis Tondelier,[b]
Bernard Geffroy,[b,c] Urelle Biapo,[b] Rémi Métivier,[d] Olivier Jeannin,[a] Joëlle Rault-Berthelot,[a] and
Cyril Poriel[a] ***

a: UMR CNRS 6226- Université Rennes 1- 35042 Rennes-France;

 b: LPICM, CNRS, Ecole Polytechnique, Université Paris Saclay, 91128, Palaiseau, France;

c: LICSEN, NIMBE, CEA, CNRS, Université Paris-Saclay, CEA Saclay 91191 Gif-sur-Yvette
Cedex, France;

d: UMR CNRS 8531-PPSM, ENS Cachan - 94235 Cachan, France

*e-mail: cyril.poriel@univ-rennes1.fr

Abstract:

The present works report the first structure-properties relationship study of a key class of
organics semiconductors, ie the four spirobifluorene positional isomers possessing a *para, meta*
or *ortho* linkage. The remarkable and surprising impact of the ring bridging and of the linkages
on the electronic properties of the regioisomers has been particularly highlighted and
rationalized. The impact of the ring bridging on the photophysical properties has been stressed
with notably the different influence of the linkages and the bridge on the singlet and triplet
excited states. The first member of a new family of spirobifluorenes substituted in position 1,
which presents better performances in blue Phosphorescent OLEDs than those of its
regioisomers is reported. These features highlight not only the great potential of 1-substituted
spirobifluorenes but also the remarkable impact of regioisomerism on electronic properties.

1. INTRODUCTION

Regioisomerism, also called positional isomerism, is an important concept in organic chemistry
which can have remarkable consequences on the properties of molecules.[1] Indeed, a simple
structural modification can drastically influence the electronic and physical properties of an
organic semi-conductor (OSC), which in turn strongly modifies the performance and stability of

the corresponding electronic device. Although very promising, this concept remains nevertheless barely used in optoelectronics. Recently, our groups have reported the remarkable impact of regioisomerism to finely tune the singlet and triplet energies of dihydroindenofluorenes leading to highly efficient optoelectronic devices.[1, 2] Similarly, Haley and co-workers have shown the impact of the regioisomerism on the electronic properties of a promising family of antiaromatic indenofluorene derivatives.[3, 4] Spiro configured compounds constitute one of the most important class of OSCs. Indeed, since the discovery of the 'spiro concept', the 9,9'-spirobifluorene (SBF) has become a central molecular scaffold in organic electronics.[5-9] 2-Substituted SBFs are in this context the most developed class of SBF-based polymers and oligomers. The *para* linkage between the pendant substituent in position 2 and the constituted phenyl ring of the fluorene ensures a good delocalization of π-electrons, essential to develop efficient fluorophores. However, in recent years, the growing necessity to design efficient host materials for blue Phosphorescent Organic Light-Emitting Diodes (PhOLED)[10, 11] has led to a huge demand of new generations of SBF based materials with wide energy gap (ca 4 eV) and hence a restricted π-conjugation. Indeed, in order to obtain a high triplet energy (E_T), key feature in the design of host materials for blue PhOLEDs, which are still the weakest link of this technology, it is mandatory to restrict the π-electrons delocalization within the OSC. This π-conjugation disruption has been successfully investigated with *ortho* linked SBFs (substitution in position 4)[12-16] and *meta* linked SBFs (substitution in position 3),[2, 17-20] leading to high performance blue PhOLEDs. However and despite the recent very high efficiency devices obtained by Jiang *et al,*[17] and by our groups[15] only few examples of 3- and 4-substituted SBFs have been described to date and more importantly no rational structure-properties relationship studies have been reported on SBF regioisomerism. Such studies are nevertheless the foundation of materials design for electronics. Thus, the combination of steric hindrance (*ortho* position) and electronic decoupling (*meta* position) found in 1-substituted SBF, has never been studied and could nevertheless be the best way to obtain high E_T OSCs based on the SBF scaffold. We hence aim to report herein not only the first example of a 1-substituted SBF, namely 1-phenyl-SBF **1** (Chart 1), but also a detailed study describing the impact of SBF regioisomerism on the electronic properties and device efficiency.
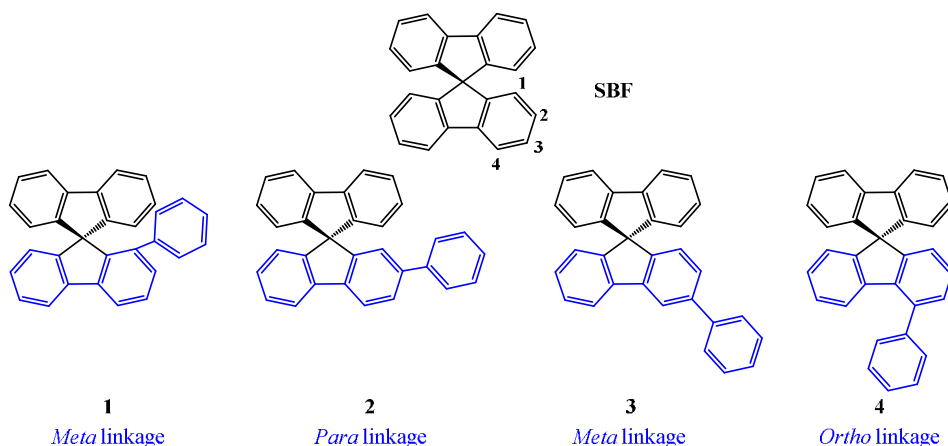

Chart 1. SBF and the four positional isomers of phenyl substituted SBFs

This work reports hence the first structure-properties relationship study of the four SBF positional isomers (substituted with a phenyl ring) namely 2-phenyl-SBF **2** possessing a *para*

linkage,[21] 1-phenyl-SBF **1** and 3-phenyl-SBF **3** both possessing a *meta* linkage and 4-phenyl-SBF **4** possessing an *ortho* linkage,[22] Chart 1. Thanks to a comparison with the structurally fluorene analogues, this work provides a foundation on the impact of SBF regioisomerism on the electronic properties. This study notably shows the surprising consequences of the ring bridging on the π-conjugation and the different influence of the linkages and the bridge on the singlet and triplet excited states. This approach has allowed the design of the first member (**1**) of a new family of OSCs, which possesses a very high E_T (2.86 eV), one of the highest reported for SBF-based materials. As a first electronic application, **1** has been used as a host in blue PhOLEDs with higher performance than those using its regioisomers, highlighting the great potential of this family of OSCs.

RESULTS AND DISCUSSIONS

The synthesis of **2** and **4** has been previously described in literature,[21, 22] that of **1** and **3** is described in Scheme 1. The synthesis of **1** (Scheme 1, Top) starts with the synthesis of the key fluorenone **c1**, substituted in position 1 with an iodine atom. First, the Susuki-Myaura cross-coupling between 3-bromoaniline and (2-(ethoxycarbonyl)phenyl)boronic acid in the presence of Pd(dppf)Cl$_2$ as catalyst and potassium carbonate as base provides the corresponding biphenyl **a1** bearing a carboxylate and an amine function (yield 41%). The electrophilic intramolecular cyclization of the ester **a1** was then performed in methanesulfonic acid at high temperature (130°C), providing the fluorenone **b1** substituted in position 1 (43% yield). One can note that the reaction also provides the fluorenone substituted in position 3. The regioselectivity has not been studied in detail herein but preliminary works seem to show that the temperature and the nature of the solvent have an important effect as previously reported in literature for similar aromatic electrophilic substitutions.[23, 24] The substitution of the amine by an iodine atom is then performed through a Sandmeyer reaction on fluorenone **b1** providing the 1-iodofluorenone **c1** with 75% yield. We note that compound **c1** reported herein widens the scope of substituted fluorenone isomers as key building blocks for the synthesis of spiro derivatives for organics electronics.[14, 25-27] Pd Catalysed cross-coupling (Pd(dba)$_2$, PCy$_3$, KF, DMF, 130°C) between **c1** and phenylboronic acid then gives the 1-phenylfluorenone **d1** with a high yield of 85%. Thus, despite a sterically hindered environment, incorporation of pendant substituents in position 1 through Pd Catalysed cross-coupling is an interesting strategy to obtain 1-substituted fluorenone derivatives. Finally, the synthesis of **1** was then carried out through a classical two-step procedure. The lithium-bromine exchange of 2-bromobiphenyl with *n*-butyllithium at low temperature, followed by addition of fluorenone **d1** afforded the corresponding fluorenol (not isolated) and further involved in an intramolecular cyclization reaction (AcOH/HCl) to provide the expected 1-phenyl spirobifluorene **1** with an overall yield of 38% over the two steps. This synthetic strategy is straightforward and provides to the best of our knowledge the first example of a 1-substituted SBF for organic electronics.

The synthesis of **3** (Scheme 1, bottom) follows a similar strategy involving the synthesis of the 3-bromofluorenone **d3** as key fragment. Thus, (2-Aminophenyl)(4-bromophenyl)methanone, possessing an amine function in α position of the ketone, was first diazotised by conventional means and then reacted in situ to form a carbon-carbon bond leading to the corresponding fluorenone backbone.[28] 3-bromofluorenone **c3** is thus obtained with 55% yield. Susuki-Myaura cross-coupling between **c3** and phenylboronoic acid (Pd(dppf)Cl$_2$, K$_2$CO$_3$, DMF, 150°C) leads to the formation of 3-phenylfluorenone **d3** with a high yield of 89%. Finally, following the same

sequence than that above exposed, the 3-phenyl substituted SBF **3** is obtained with a very high yield of 90% (2 steps).
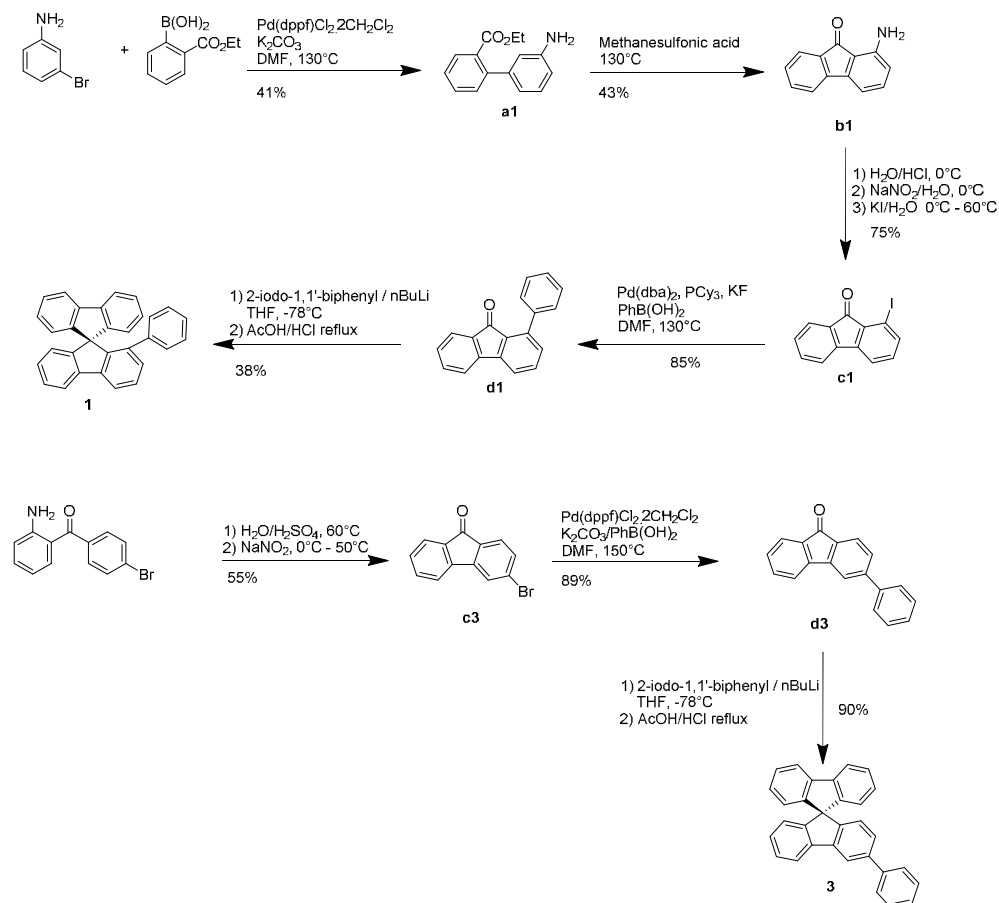
Scheme 1. Synthetic routes to **1** and **3**.

The structural arrangement of **1-4** obtained by X-Ray diffraction is depicted in Figure 1. The most important structural feature is the relative position of the pendant phenyl ring with respect to the fluorene. First, **2** presents a dihedral angle between the mean plane of the pendant phenyl ring and that of its attached phenyl ring of the fluorene of 37.4° (Figure 1, top right). This angle, characteristic of a non-encumbered phenyl/fluorene *para* linkage,[29] maximises the conjugation between the two fragments. In **3**, the *meta* linkage leads to an even smaller dihedral angle of 34.2° between the fluorene and its attached phenyl ring (Figure 1, bottom left). In **4**, the presence of the pendant phenyl ring in *ortho* position of the biphenyl linkage leads to an impressive enhancement of the dihedral angle, recorded at 51.2° (Figure 1, bottom right).[21] This structural feature, assigned to the steric interaction between the hydrogen atoms in *ortho* position of the pendant phenyl ring and that of the fluorenyl core is at the origin of the partial π-conjugation breaking of 4-substituted SBFs.[22] In **1**, this dihedral angle appears to be impressively larger reaching 75.4° (Figure 1, top left) for one molecule and 66.7° for the other (2 molecules are indeed present in the asymmetric unit, see SI). This structural particularity is the consequence of

4

the substitution in *ortho* position of the spiro carbon, which leads to a sterically hindered environment due to the presence of the cofacial fluorene. Indeed, very short C/C distances are measured between carbon atoms of the non-substituted fluorene and those of the pendant phenyl ring (3.25 and 3.31 Å for one molecule and 3.20, 3.29 and 3.33 Å for the other molecule, see SI). These C/C distances are shorter than the sum of their Van der Waals radii (3.4 Å) and translate strong interactions between the two cofacial fragments as confirmed by the electrostatic potential surface obtained by molecular modelling (see SI). Thus, in the four SBF isomers, the position of the phenyl ring leads to different steric hindrances with the substituted or the non-substituted fluorene. This structural feature will be one of the key parameters involved in the electronic properties (see below).
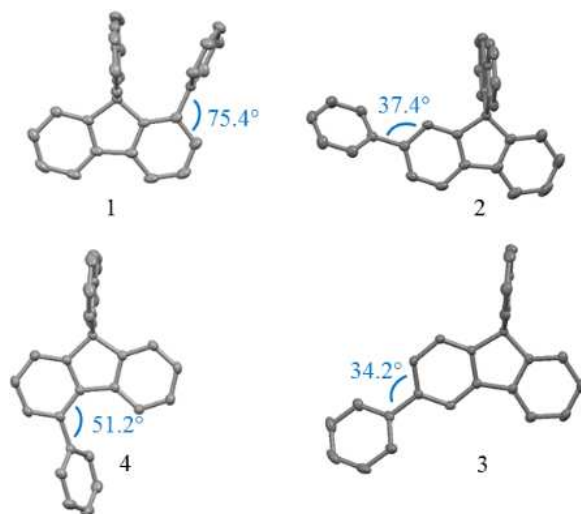

Figure 1. ORTEP drawing of **1-4** (ellipsoid probability at 50 % level).

	1	2	3	4	SBF
λ_{abs} $(\epsilon)^a$ (nm) $(\times 10^4$ L mol^{-1} cm^{-1})	298 (0.98) 309 (1.66)	296 (2.44) 308 (2.31) 319 (1.60)	297 (0.92) 310 (1.49) 316 (0.64)	297 (1.07) 309 (1.49)	297 (0.72) 308 (1.45)
λ_{em}^a (nm)	313, 323	334, 350	332, 343	359	310, 323
QY^a	0.61	0.87	0.74	0.42	0.40
τ (ns)^a	5.16	1.56	5.74	4.20	4.60
k_r ($\times 10^8$) (s^{-1})	1.22	5.60	1.29	1.00	0.87
k_{nr} ($\times 10^8$) (s^{-1})	0.72	0.83	0.45	1.40	1.30
HOMO (eV)	El^b -5.94	-5.86	-5.94	-5.95	-5.95
	Calc^d -6.00	-5.90	-5.97	-6.02	-6.03
LUMO (eV)	El^b -1.73	-1.99	-1.77	-1.87	-1.74
	Calc^d -1.32	-1.55	-1.34	-1.38	-1.30
ΔE (eV)	Opt^c 3.95	3.70	3.78	3.82	3.97
	El^b 4.21	3.87	4.17	4.08	4.21
E_T (eV)	Opt^e 2.86	2.56	2.83	2.78	2.88
	Calc^f 2.65	2.38	2.64	2.57	2.67
τ (s)^e	5.8	3.3	5.4	4.7	5.3

Table 1. Electronic data of **1-4** and **SBF**

[a.] in cyclohexane, [b.] from CVs, [c.] from UV-Vis spectra, [d.] from DFT calculations, [e.] in 2-Me-THF. [f.] from TD-DFT calculations

The UV-Vis absorption spectra of the SBF regioisomers are presented Figure 2, top left and time-dependant density functional theory (TD-DFT, Figure 3) calculations have been performed

using the B3LYP functional and the extended 6-311+G(d,p) basis set on the optimized geometry of S0 (B3LYP/6-31G(d). The unsubstituted **SBF** exhibits two characteristic bands at 297 and 308 nm corresponding to $\pi-\pi*$ transitions (See TD-DFT calculations in SI).[22] The four phenyl-substituted SBF isomers all display these two thin bands (Figure 2) at a similar wavelength. In addition to these bands, **2** displays an extra and large band centred at 319 nm. This band clearly signs an extension of the $\pi-$conjugation from fluorene in **SBF** to phenyl-fluorene in **2** and is assigned to an HOMO→LUMO transition (with both orbitals centred on the phenyl-fluorene fragment), possessing a high oscillator strength (f=0.59, Figure 3, Top right). This extension of conjugation is due to the combination of two parameters: the *para* linkage and the small dihedral angle (Figure 1) formed between the phenyl and the fluorene. Instead of this large band at 319 nm, the spectrum of **4** only presents a weak tail between 309 and 325 nm assigned to an HOMO→LUMO transition with a weak oscillator strength (f=0.11, Figure 3, bottom right). The presence of this tail reflects a certain degree of π-conjugation between the fluorene moiety and the phenyl ring, induced by the *ortho* linkage. There is however a strong π-conjugation disruption in **4** due to the large angle formed between the fluorene and the phenyl in C4. Indeed, the calculated electronic density accompanying this first electronic excitation shows that this pendant phenyl ring is involved with a weak contribution (see SI). The *meta* linkage found in both **1** and **3** leads to very different results. Indeed, in **3**, we note the presence of a large band at 316 nm, very similar to that observed for **2**, and assigned in the light of TD-DFT to a transition possessing two major contributions, HOMO→LUMO and HOMO→LUMO+2 (f=0.15, Figure 3, bottom-left). This band at 316 nm translates a clear extension of the $\pi-$conjugation with nevertheless a molar absorption coefficient 2.5 times lower than that observed for the *para* isomer **2** (**2**: $\varepsilon_{319nm}=1.6\times10^4$ L mol^{-1} cm^{-1}; **3**: $\varepsilon_{316nm}=0.64\times10^4$ L mol^{-1} cm^{-1}). However, the presence of this band appears to be very surprising in the light of literature. Indeed, the absorption spectrum of the *meta* terphenyl (analogue of **1** and **3** but without the bridge) possesses a λ_{max} at 246 nm, strongly blue shifted compared to that of its regioisomer, the *para* terphenyl (analogue of **2**), λ_{max} = 277 nm.[2] This π-conjugation disruption observed for *meta* terphenyl finds its origin in the shape and distribution of the molecular orbitals involved (small contributions are indeed found on *meta* carbons).[30] Indeed, it is admitted that there is a better delocalisation of π-electrons following the *para/ortho/meta* sequence and numbers of studies have tried to elucidate the origin of the restricted π-conjugation between *para, ortho* and *meta* substituted oligophenylenes.[30-36] In our case, it is clear that **3** displays a different behaviour compared to its building block *meta* terphenyl as it presents a relatively intense degree of conjugation between the phenyl and the fluorene. Thus, the 'linkage' effect cannot explain by itself this feature and other parameters should be invoked. We believe that the $\pi-$conjugation extension of **3** finds its origin in the electron donating effect of the bridge, herein the spiro carbon. Indeed, the spiro carbon may increase the electron density in its *para* position that is in C3 allowing the π-conjugation extension.[17]
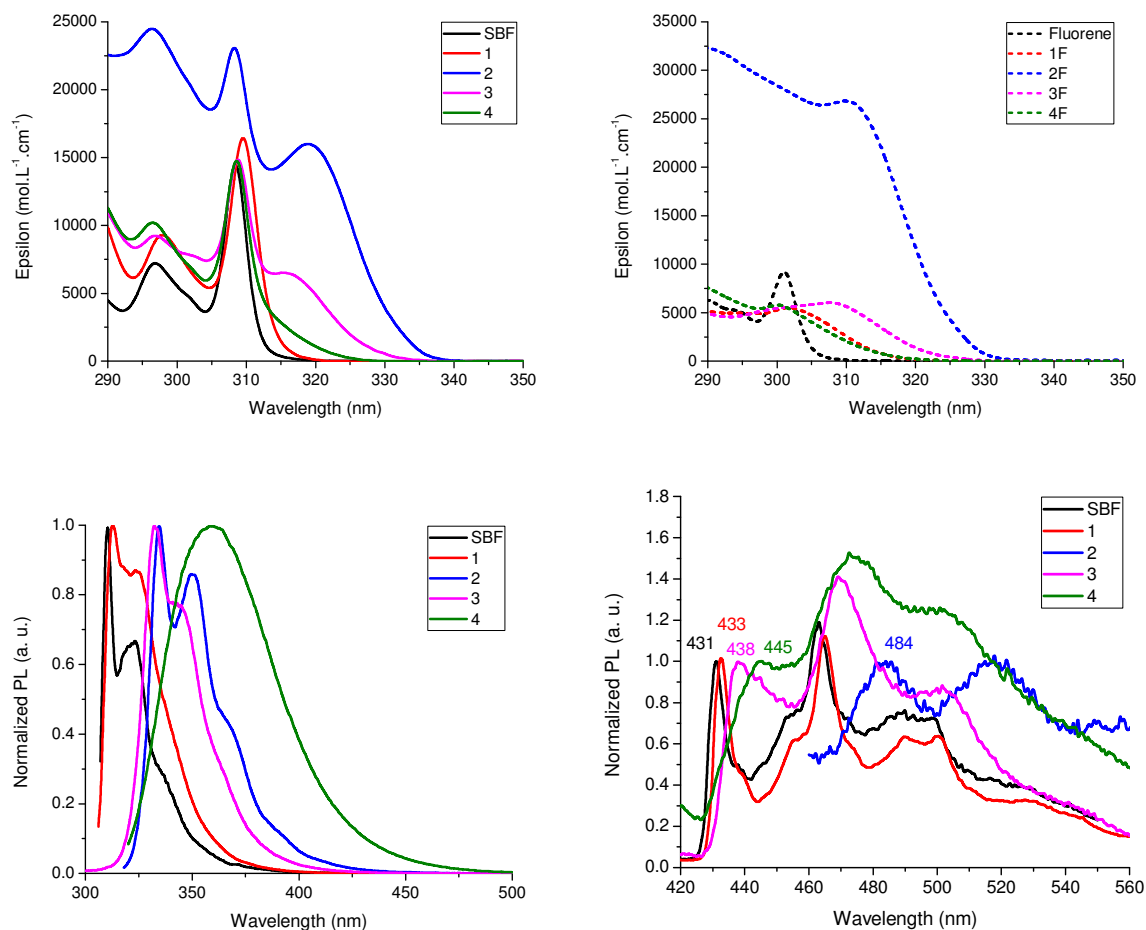
Figure 2. Top: Absorption in cyclohexane of **1-4** and **SBF** (left) and **1F-4F** and **F** (right); bottom: Emission at rt (cyclohexane, left) and at 77 K (2-Me-THF, right) of **1-4** and **SBF**

To unravel this 'ring bridging' effect, we have chemically modified the bridge through the synthesis of the related fluorene analogues (see SI), namely 1-phenylfluorene (**1F**), 2-phenylfluorene (**2F**), 3-phenylfluorene (**3F**), 4-phenylfluorene (**4F**), possessing a methylene bridge instead on the spirofluorene bridge. As observed for **3**, the absorption spectrum of the *meta* isomer **3F** surprisingly displays a large band, λ_{max} =308 nm, at an almost identical wavelength than that observed for the *para* isomer **2F**, λ_{max} =310 nm (**3F**: ε_{308nm}=0.60×10^4 L mol^{-1} cm^{-1}; **2F**: ε_{310nm}=2.68×10^4 L mol^{-1} cm^{-1}, Figure 2, Top right). This large band translates the π−conjugation extension and the clear difference observed between the absorption spectra of the two *meta* isomers, **3F** and **1F**, sheds light on the key role played by the bridge. Thus, *meta* isomers **3F** and **3** display a similar behaviour showing a surprising conjugation extension, less intense than the *para* analogues **2** and **2F** but more intense than their *ortho* isomers **4F** and **4**, hence confirming the remarkable impact of the bridge on the optical properties. Thus, the

8

rigidification of the *meta* terphenyl core by one bridge cancels, at least partially, the effect of the linkages on the conjugation length, which appears as an interesting way to tune the electronic properties of bridged oligophenylenes.

The other *meta*-linked SBF **1** displays a very different absorption spectrum almost identical to that of **SBF** with a main thin band at 309 nm and no trace of extended conjugation at higher wavelengths. TD-DFT of **1** reveals for this band two main transitions (HOMO→LUMO and HOMO→LUMO+1, Figure 3, Top left) all involving only the fluorene fragment with no electronic density found on the phenyl unit (see also the calculated electron density changes in SI). This feature highlights a strong similitude with the transitions observed for **SBF**. Thus, the complete π-conjugation breaking of **1** finds its origin not only in the *meta* linkage, which cannot completely break the conjugation as exposed above for **3** but also in the very large dihedral angle measured between the phenyl unit and the fluorene. This large angle is caused by the presence of the spiroconjugated fluorene, which strongly restricts the rotation of the phenyl ring. Removing this bulky spirofluorene such as in the fluorene analogue **1F** above mentioned, confirms its importance as one can note a long tail in the absorption of **1F** (Figure 2, top right) reflecting a clear conjugation between the phenyl and the fluorene moiety (see the calculated electron density changes in SI). It is noteworthy that *meta* isomer **1F** and *ortho* isomer **4F** possess an almost identical absorption spectrum (**1F**: $\varepsilon_{302nm}=0.55\times10^4$ L mol^{-1} cm^{-1}; **4F**: $\varepsilon_{300nm}=0.58\times10^4$ L mol^{-1} cm^{-1}, Figure 2, top right), confirming that the bridge rigidification cancels the effect of the linkages on the conjugation length. There is hence a better delocalisation following the **2-/3-/4-/1-** sequence which translates into an opening of the optical gap ΔE_{opt} from **2** (3.70 eV) to **1** (3.95 eV). Thus, the most efficient conjugation is found for **2** and **3**, which do not present any steric congestion highlighting its importance whatever the linkages involved.
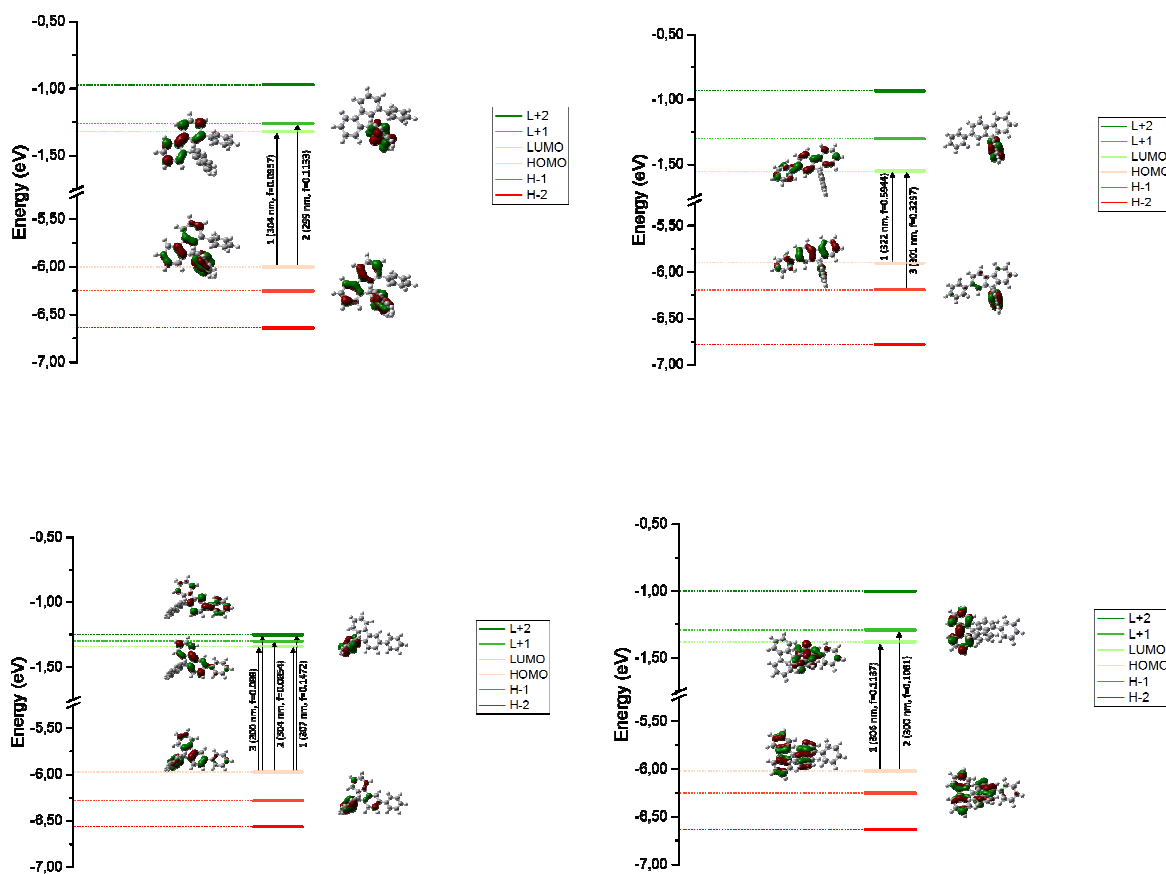
Figure 3 Representation of the energy levels and the main molecular orbitals involved in the electronic transitions of **1** (top left), **2** (top right), **3** (bottom left) and **4** (bottom right) obtained by TD-DFT B3LYP/6-311+G(d,p), shown with an isovalue of 0.04 [e bohr^{-3}]$^{1/2}$.

The properties of **1-4** in their excited state confirm the key steric and electronic roles of the spiro bridge. In fluorescence (Figure 2, bottom left), the same trend as that exposed above is observed for all dyes (except **4** which is a very particular case not discussed herein). Indeed, **2** and **3** possess an almost identical emission spectrum, which are the most red-shifted in the series due to their extended conjugation (λ_{max}=334 and 332 nm *resp.*). This result, although in full accordance with that exposed above in absorption appears again very surprising as the *meta* linkage of **3** should strongly restrict the π-conjugation compared to the *para* linkage of **2**.[22,25] This is again the consequence of the spiro bridge in *para* position of the phenyl ring. Both fluorophores **2** and **3** also display a high quantum yield (87 and 74 % *resp.*), indicating weak non-radiative pathway from S_1 to S_0. Thus, from a spectral shape point of view, *para* and *meta* linkages are noticeably almost indistinguishable. Important differences can be nevertheless found in the activation/deactivation processes. Indeed, the fluorescence decay curves of **2** provides a single lifetime of 1.56 ns, which is noticeably shorter than that of **3** (5.74 ns). The radiative rate constant (k_r) of **2** is calculated to be 5.6×10^8 s^{-1}, that is about 4 times that of **3** (1.29×10^8 s^{-1}).

This feature is in good agreement with the oscillator strengths difference observed for the first electronic transitions (f=0.59 for **2** and 0.15 for **3**). However, the non-radiative rate constant (k_{nr}) of **2**, (k_{nr} =0.83×10^8 s^{-1}) is twice that of **3** (k_{nr} =0.45×10^8 s^{-1}), this feature showing that vibrational deactivation pathways are more favourable for the former than for the latter despite their identical environment. Thus, despite **2** and **3** possessing a similar quantum yield and spectrum shape, they nevertheless present very different radiative and non-radiative constants, highlighting the importance of the linkages on the photophysical processes. Remarkably, **1** displays a blue-shifted emission spectrum (λ_{max}= 313 nm) compared to that of **3** despite the identical *meta* linkages of both molecules. The spectrum of **1** is even almost identical to that of its building block **SBF**, completely erasing the effect of the pendant phenyl ring on the π-conjugation pathway at the excited state. The quantum yield of **1** is nevertheless higher than that of **SBF** (0.61 and 0.40 *resp.*), indicating that 1-substituted SBFs are very efficient near UV emitters. The higher quantum yield of **1** compared to that of **SBF** is due to a combination of a higher k_r (1.22×10^8 s^{-1} for **1** and 0.87×10^8 s^{-1} for **SBF**) and a smaller k_{nr} (0.72×10^8 s^{-1} for **1** and 1.30×10^8 s^{-1} for **SBF**). If one compares the two *meta* substituted isomers **1** and **3**, it is noteworthy that the loss of quantum yield in case of **1** mainly results in more efficient internal conversion processes (k_{nr} of **3** smaller than k_{nr} of **1**) and not in much lower electronic transition moment (identical k_r for **1** and **3**). Thus, the absorption and emission spectra at room temperature follow the surprising same trend. This is not the case at 77 K.

At 77 K, the emission spectra of **1-4** present a well resolved phosphorescence contribution, with a first band centred at 431 nm for **1**, 483 nm for **2**, 438 nm for **3** and 445 nm for **4** (Figure 2, bottom right). The corresponding E_T of **1-4** were thus respectively estimated at ca 2.86, 2.56, 2.83 and 2.78 eV. Due to the π-conjugation disruption, the *meta*-substituted terphenyl core of **1** and **3** leads to an increase of the E_T compared to the *para*-substituted terphenyl core of **2** and to a lesser extent to that of the *ortho*-substituted terphenyl core of **4**. *Para, ortho* and *meta* terphenyls, analogue of **1-4** but without any bridge, follow the same trend with E_T of 2.55, 2.67 and 2.82 eV respectively.[2, 37] Two important features need to be stressed out: (i) The E_T of **1** (2.86 eV) is almost identical to that of **SBF** (E_T=2.88 eV) confirming that the pendant phenyl has no influence on the T1 state (Figure 4 bottom), which is a key point for further use as host in blue PhOLED (see below), (ii) The emission from T1 state follows a classical *para/ortho/meta* sequence (E_T increases as follows **2/4/3/1**), being hence different to that of S1-S0. Thus, and oppositely to our observations in absorption and fluorescence, the nature of the linkage fully drives the E_T values. Indeed, the triplet exciton of **3** is localized along the substituted fluorene with no contribution of the pendant phenyl (Figure 4, bottom), maintaining hence a high E_T of 2.83 eV. Oppositely, the delocalization of the triplet exciton of **4** presents a significant contribution of the pendant phenyl, which in turn decreases the E_T to 2.78 eV. This feature is very different to that observed for HOMO and LUMO distribution (see below) and indicate the peculiar behaviour of these isomers. Thus, the singlet and triplet energies follow different trends with a remarkable different contribution of the pendant phenyl. The bridge seems hence to have a strong impact in the singlet state energy whereas the triplet state energy is fully driven by the nature of the linkages. Finally, radiative deactivation of the triplet state of **SBF** and **1-4** has been measured and appears to be very slow under these experimental conditions: the phosphorescence decay was measured and the lifetime of the T_1 state of **1** and **3** was found to be 5.8 sec and 5.4 sec, respectively. Thus, the *meta* linkages of **1** and **3** lead to the longer lifetimes very similar to that measured for **SBF**. The *para* linkages of **2** have an important influence on the photophysical properties of the T_1 state, since its lifetime (3.3 sec) was found to be shorter than its *para* and

ortho isomers (4.7 s for **4**), highlighting hence the impact of the nature of the linkages on the phosphorescence lifetimes.
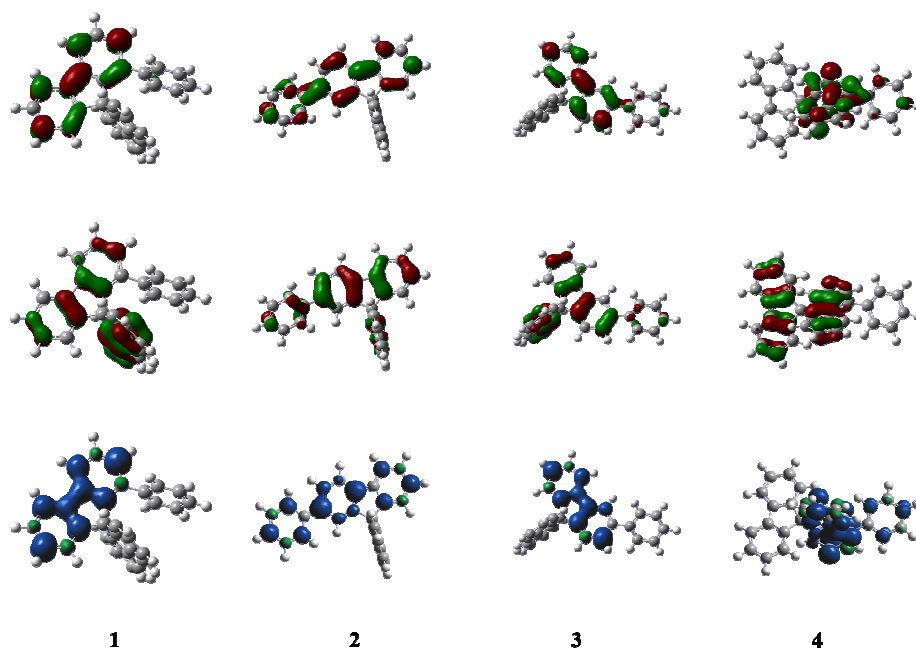

Figure 4. Frontier molecular orbitals (Top: LUMO, Middle: HOMO) and SDD triplet (down) with isovalues of 0.04 and 0.004 respectively

The cyclic voltammetry (CV) of **1-4** allows to determine their HOMO energies[38] at -5.94, -5.86, -5.94 and -5.95 eV respectively (Figure 5, Right). Thus, despite their phenyl substitution, **1**, **3** and **4** possess the same HOMO energy than that of **SBF** (-5.95 eV). This is in accordance with the electronic distribution of their HOMO (Figure 4-middle), which does not (or weakly for **3**) present any density on the pendant phenyl ring due to the phenyl/fluorene steric hindrance for **1** and **4** and to the *meta* conjugation for **3**. The HOMO of **2** (-5.86 eV) which presents an electron density delocalized through the phenyl/fluorene fragment is obviously the highest in the series. In the fluorene series, a different sequence is detected. Indeed, the HOMO levels of **1F-4F** are respectively recorded at -5.94, -5.72, -5.89 and -5.93 eV (See CVs and molecular modelling in SI). Oppositely to the SBF series, the HOMO of **3F** is significantly higher than that of **1F** and **4F**. This is in accordance with the electronic density detected on the pendant phenyl ring of **3F** and highlights that the steric hindrance found in **1F** and **4F** is more efficient than the nature of the linkage to restrain the electronic density within the fluorene core. This important difference observed between the F and SBF series indicates that the bridge (methylene vs spirofluorene) has a considerable impact on the HOMO distribution and energy levels. The cathodic explorations (Figure 5, Left) have again revealed a different behaviour in each series. In the SBF series, the LUMO energy of **1** (-1.73 eV) is almost identical to that of **SBF** (-1.74 eV), indicating, as for the HOMO, that the phenyl ring in position 1 does not influence the LUMO energy (Figure 4, top). However, **3** and **4** display a different behaviour with a deeper LUMO respectively evaluated at -1.77 eV and -1.87 eV translating the non-negligible influence of the phenyl unit on the LUMO energy. This is particularly pronounced for **4**, which presents a significant contribution of the phenyl ring in the LUMO distribution, which is not the case for its HOMO level. Thus, the

12

phenyl ring has a different influence on the benzenoidal HOMO/quinoidal LUMO distribution depending of the regioisomer involved. This significantly different influence of the phenyl ring over HOMO/LUMO levels is also observed in the fluorene series, this feature being hence assigned to the ring bridging. Thus, the LUMO levels of **1F-4F** are respectively recorded at -1.77, -1.92, -1.71 and -1.82 eV. We particularly note that there is a strong contribution of the phenyl ring in the LUMO of **1F** (See SI), which strongly decreases its energy compared to that of **F**. This is a significant difference with the LUMO of **1**, which only implies the fluorene, highlighting the key steric role of the spiro bridge.
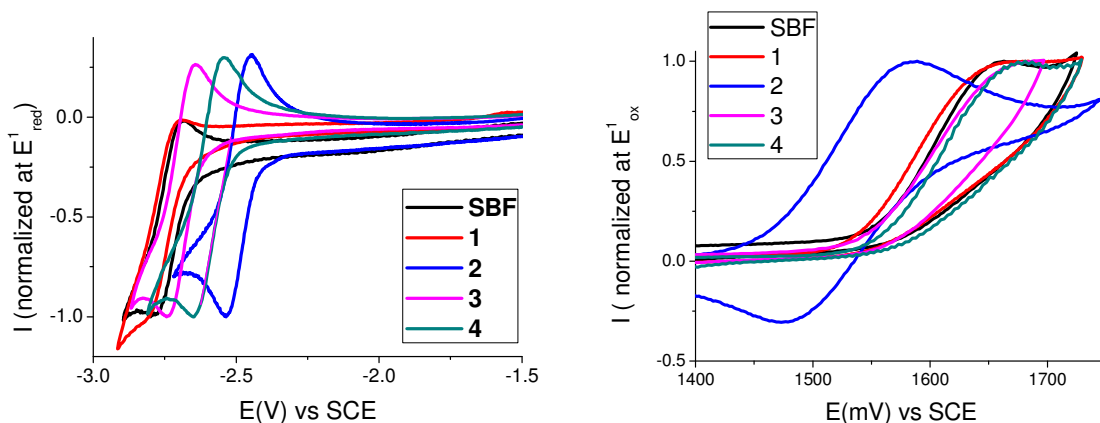

Figure 5. Cyclic Voltammetry (CV) of **1-4** and **SBF** recorded in DMF/Bu$_4$NPF$_6$ 0.1 M (reduction, left) and in dichloromethane/Bu$_4$NPF$_6$ 0.2 M (oxidation, right).Sweep-rate: 100 mV/s. Platinum working electrode. All CVs are normalized at the peak potential of the reduction (left) or oxidation (right) process.

In order to finally explore the potential of the 1-substituted SBF family in electronics and more generally the impact of regioisomerism on device performance, **1**, **3** and **4** have been used as host in blue PhOLEDs containing very low amount of FIrpic (5%, see structure in SI). Indeed, **2** cannot be used (E$_T$=2.56 eV), since in order to insure efficient energy transfers within the emissive layer,[39] the host should possess a higher E$_T$ than that of the blue phosphor FIrpic (E$_T$=2.62 eV).[40] The device using **3** presents a Current Efficiency (CE) of 12.8 cd/A, a Power Efficiency (PE) of 4.36 lm/W and an External Quantum Efficient (EQE) of 4.7 % (at 10 mA.cm^{-2}). *Ortho* substituted **4** displays slightly higher performance with an EQE of 5.5 %, a CE of 14.3 cd/A and a PE of 5.8 lm/W. The performance of the *meta* substituted isomer **1** appears to be the highest in the series with an EQE of 5.9 % and corresponding CE and PE of 15.9 cd/A and 5.9 lm/W respectively. As the device architecture is identical, the different performance, despite small, can be only imputed to the efficiency of the host and more precisely to the position of the phenyl ring within the molecular structure (see PhOLED data of **1**, **3** and **4** in SI). In the light of these performances, the 1-substituted SBF scaffold appears promising to host blue phosphors. All the electroluminescent spectra (see SI) exclusively present the emission of FIrpic indicating an efficient energy transfer cascade. Thus, this first electronic application of a 1-substituted SBF shows a good confinement of the excitons within the emitting layer, which is a crucial point for optoelectronics. It should be stressed that these blue PhOLEDs performances remain modest compared to the best recently reported for pure hydrocarbons.[17] However, with a more accurate

design (incorporation of donor and/or acceptor units),[15, 41] device performance could be easily increased and this new family of 1-substituted SBF can play an interesting role in the future.

CONCLUSION

To summarize, this work reports the first rational study on SBF regioisomerism, highlighting the chief influence of the bridge and of the linkages on the electronic properties. Of particular interest, the impact of the ring bridging on the photophysical properties has been evidenced with notably the different influence of the linkages and the bridge on the singlet and triplet excited states. The first member of a new family of SBFs substituted in position 1 is reported, which possesses a very high triplet energy and presents better performance in blue PhOLEDs than those of its regioisomers. These features highlight not only the potential of 1-substituted SBFs but also the remarkable impact of regioisomerism on electronic properties.

Keywords: spirobifluorene, regioisomerism, blue PhOLED, $\pi-$conjugation, ring bridging

Supporting Information

Details on material and methods, electrochemical properties, structural properties, photophysical properties, molecular modelling, device fabrication and characterization, copy of NMR spectra.

REFERENCES

[1]M. Romain, D. Tondelier, J.-C. Vanel, B. Geffroy, O. Jeannin, J. Rault-Berthelot, R. Métivier, C. Poriel, *Angew. Chem. Int. Ed.* **2013**, *52*, 14147-14151.
[2]M. Romain, S. Thiery, A. Shirinskaya, C. Declairieux, D. Tondelier, B. Geffroy, O. Jeannin, J. Rault-Berthelot, R. Métivier, C. Poriel, *Angew. Chem. Int. Ed.* **2015**, *54*, 1176-1180.
[3]A. G. Fix, D. T. Chase, M. M. Haley, in *Top. Curr. Chem* (Eds.: J. S. Siegel, Y.-T. Wu), Springer-Verlag Berlin Heidelberg, **2014**, pp. 159-195.
[4]A. G. Fix, P. E. Deal, C. L. Vonnegut, B. D. Rose, L. N. Zakharov, M. M. Haley, *Org. Lett.* **2013**, *15*, 1362-1365.
[5]T. P. I. Saragi, T. Spehr, A. Siebert, T. Fuhrmann-Lieker, J. Salbeck, *Chem. Rev.* **2007**, *107*, 1011-1065.

[6] L.-H. Xie, J. Liang, J. Song, C.-R. Yin, W. Huang, *Current Organic Chemistry* **2010**, *14*, 2169-2195.

[7] X.-F. Wu, W.-F. Fu, Z. Xu, M. Shi, F. Liu, H.-Z. Chen, J.-H. Wan, T. P. Russell, *Adv. Funct. Mat.* **2015**, *25*, 5954-5966.

[8] J. Yi, Y. Wang, Q. Luo, Y. Lin, H. Tan, H. Wang, C.-Q. Ma, *Chem. Commun.* **2016**, *52*, 1649-1652.

[9] N. J. Jeon, H. G. Lee, Y. C. Kim, J. Seo, J. H. Noh, J. Lee, S. I. Seok, *J. Am. Chem. Soc.* **2014**, *136*, 7837-7840.

[10] K. S. Yook, J. Y. Lee, *Adv. Mater.* **2012**, *24*, 3169-3190.

[11] K. S. Yook, J. Y. Lee, *Adv. Mater.* **2014**, *26*, 4218-4233.

[12] C. Fan, Y. Chen, P. Gan, C. Yang, C. Zhong, J. Qin, D. Ma, *Org. Lett.* **2010**, *12*, 5648-5651.

[13] Z. Jiang, H. Yao, Z. Zhang, C. Yang, Z. Liu, Y. Tao, J. Qin, D. Ma, *Org. Lett.* **2009**, *11*, 2607-2610.

[14] S. Thiery, D. Tondelier, C. Declairieux, B. Geffroy, O. Jeannin, R. Métivier, J. Rault-Berthelot, C. Poriel, *J. Phys. Chem. C* **2015**, *119*, 5790–5805.

[15] S. Thiery, D. Tondelier, B. Geffroy, E. Jacques, M. Robin, R. Métivier, O. Jeannin, J. Rault-Berthelot, C. Poriel, *Org. Lett.* **2015**, *17*, 4682-4685.

[16] C. Quinton, S. Thiery, O. Jeannin, D. Tondelier, B. Geffroy, E. Jacques, J. Rault-Berthelot, C. Poriel, *ACS Appl. Mater. Interfaces.* **2017**, *in press DOI: 10.1021/acsami.6b14285*

[17] L.-S. Cui, Y.-M. Xie, Y.-K. Wang, C. Zhong, Y.-L. Deng, X.-Y. Liu, Z.-Q. Jiang, L.-S. Liao, *Adv. Mater.* **2015**, *27*, 4213-4217.

[18] M.-M. Xue, Y.-M. Xie, L.-S. Cui, X.-Y. Liu, X.-D. Yuan, Y.-X. Li, Z.-Q. Jiang, L.-S. Liao, *Chem. Eur. J.* **2016**, *22*, 916-924.

[19] Y. Liu, L.-S. Cui, X.-B. Shi, Q. Li, Z.-Q. Jiang, L.-S. Liao, *J. Mater. Chem. C* **2014**, *2*, 8736-8744.

[20] C. Poriel, R. Métivier, J. Rault-Berthelot, D. Thirion, F. Barrière, O. Jeannin, *Chem. Commun.* **2011**, *47*, 11703-11705.

[21] S. Thiery, C. Declairieux, D. Tondelier, G. Seo, B. Geffroy, O. Jeannin, R. Métivier, J. Rault-Berthelot, C. Poriel, *Tetrahedron* **2014**, *70*, 6337-6351.

[22] S. Thiery, D. Tondelier, C. Declairieux, G. Seo, B. Geffroy, O. Jeannin, J. Rault-Berthelot, R. Métivier, C. Poriel, *J. Mater. Chem. C* **2014**, *2*, 4156-4166.

[23] C. Poriel, J. Rault-Berthelot, D. Thirion, F. Barrière, L. Vignau, *Chem. Eur. J.* **2011**, *17*, 14031-14046.

[24] C. Poriel, F. Barrière, D. Thirion, J. Rault-Berthelot, *Chem. Eur. J.* **2009**, *15*, 13304-13307.

[25] M. Romain, M. Chevrier, S. Bebiche, T. Mohammed-Brahim, J. Rault-Berthelot, E. Jacques, C. Poriel, *J. Mater. Chem. C* **2015**, *3*, 5742-5753.

[26] D. Thirion, C. Poriel, J. Rault-Berthelot, F. Barrière, O. Jeannin, *Chem. Eur. J.* **2010**, *16*, 13646-13658.

[27] M. Romain, C. Quinton, D. Tondelier, B. Geffroy, O. Jeannin, J. Rault-Berthelot, C. Poriel, *J. Mater. Chem. C* **2016**, *4*, 1692-1703.

[28] L.-S. Cui, S.-C. Dong, Y. Liu, M.-F. Xu, Q. Li, Z.-Q. Jiang, L.-S. Liao, *Org. Electron.* **2013**, *14*, 1924-1930.

[29] D. Thirion, C. Poriel, F. Barrière, R. Métivier, O. Jeannin, J. Rault-Berthelot, *Org. Lett.* **2009**, *11*, 4794-4797.

[30] P. Guiglion, M. A. Zwijnenburg, *Phys. Chem. Chem. Phys.* **2015**, *17*, 17854-17863.

[31] S. Karaburnaliev, M. Baumgarten, N. Tyutyulkov, K. Müllen, *J. Phys. Chem.* **1994**, *98*, 11892-11901.

[32] S. Y. Hong, D. Y. Kim, C. Y. Kim, R. Hoffmann, *Macromolecules* **2001**, *34*, 6474-6481.

[33] N. Fomina, S. E. Bradforth, T. E. Hogen-Esch, *Macromolecules* **2009**, *42*, 6440-6447.

[34] C. S. Hartley, *Acc. Chem. Res.* **2016**, *49*, 646-654.

[35] J. He, J. L. Crase, S. H. Wadumethrige, K. Thakur, L. Dai, S. Zou, R. Rathore, C. S. Hartley, *J. Am. Chem. Soc.* **2010**, *132*, 13848-13857.

[36] H.-H. Huang, C. Prabhakar, K.-C. Tang, P.-T. Chou, G.-J. Huang, J.-S. Yang, *J. Am. Chem. Soc.* **2011**, *133*, 8028-8039.

[37] H. Yersin, *Highly Efficient OLEDs with Phosphorescent Materials*, Wiley-VCH:Verlag GMBH & Co. KGaA, Weinheim, **2007**.

[38] A. P. Kulkarni, C. J. Tonzola, A. Babel, S. A. Jenekhe, *Chem. Mater.* **2004**, *16*, 4556-4573.

[39] M. A. Baldo, D. F. O'Brien, Y. You, A. Shoustikov, S. Sibley, M. E. Thompson, S. R. Forrest, *Nature* **1998**, *395*, 151-154.

[40] E. Baranoff, B. F. E. Curchod, *Dalton Trans.* **2015**, *44*, 8318-8329.

[41] C. Poriel, J. Rault-Berthelot, S. Thiery, C. Quinton, O. Jeannin, U. Biapo, B. Geffroy, D. Tondelier, *Chem. Eur. J.* **2016**, *22*, 17930-17935.

TOC

2.86 eV
2.83 eV

2.78 eV

E_T

2.56 eV

300   310   320   330   340   350   λ (nm)